

Identification of Potent Small Molecule Inhibitors of SARS-CoV-2 Entry

Supplemental Material

Sonia Mediouni^{1*}, Huihui Mou^{1*}, Yuka Otsuka^{2*}, Joseph Anthony Jablonski¹, Robert Scott Adcock³, Lalit Batra³, Dong-Hoon Chung³, Christopher Rood⁴, Ian Mitchell S. de Vera⁴, Ronald Rahaim Jr.², Sultan Ullah², Xuerong Yu², Tu-Trinh Nguyen⁵, Mitchell Hull⁵, Emily Chen⁵, Thomas D. Bannister², Pierre Baillargeon², Louis Scampavia², Michael Farzan^{1†}, Susana T. Valente^{1†}, Timothy P. Spicer^{2†}

¹*Scripps Research, Department of Immunology and Microbiology, Scripps Research, Jupiter, FL 33458, USA*

²*Scripps Research, Department of Molecular Medicine, Scripps Research, Jupiter, FL 33458, USA*

³*Center for Predictive Medicine, Department of Microbiology Immunology, School of Medicine, University of Louisville, KY 40202, USA*

⁴*Department of Pharmacology and Physiology, Saint Louis University School of Medicine, St. Louis, MO 63104, USA*

⁵*CALIBR, Scripps Research, 11119 N Torrey Pines Rd, La Jolla, CA 9203, USA*

**Equal contribution*

†Co-Communicated

Supplemental tables and figures

Table S1

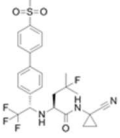
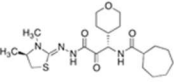
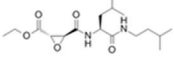
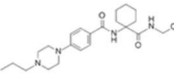
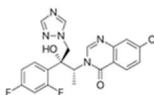
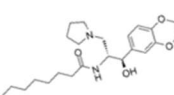
TI > 20							ReFRAMEdb		
ReFRAME	SR ID	Drug	Structure	SARS2-S (IC ₅₀ , nM)	VSV-G (IC ₅₀ , μM)	Toxicity (CC ₅₀ , μM)	TI or VSV-G/ SARS2-S	SARS- CoV-2 (IC ₅₀ , nM)	Toxicity (CC ₅₀ , μM)
	SR-806	VBV-825		88 ± 50	> 20	> 20	227.3	345.0	>10.0
	SR-132	ONO 5334		101 ± 67.9	> 20	> 20	198.0	211.0	>10.0
	SR-216	E64D		104 ± 44.2	> 20	> 20	192.3	Not included	
	SR-608	AAE581		650 ± 114	> 20	> 20	30.8	5580.0	>10.0
	SR-257	Albaconazole		459 ± 145	> 20	> 20	43.6	4140.0	>10.0
	SR-667	Eliglustat		1280 ± 408	> 20	> 20	15.6	No selected	

Table.S1. Summary of the ReFRAME compounds with a therapeutic index higher than 20. Activity of the selected compounds against the different MLV pseudotyped viruses in HEK293-ACE2 cells. Values for SARS2-S, VSV-G and toxicity are mean ± SD of 3 independent experiments. ReFRAMEdb: activity of the compounds was measured using the cytopathic effect (CPE) of the SARS CoV-2 virus infecting Vero E6 host cells. The viability of uninfected cells after exposure to hit compounds for 72 hours is measured to determine compounds cytotoxic effects. TI: therapeutic index.

Table S2

SR ID	IC ₅₀ ± S.E. (μM)	CC ₅₀ ± S.E. (μM)
SR-914	1.033 ± 0.117	28.694 ± 1.576
SR-372	0.705 ± 0.113	9.0252 ± 0.413
SR-510	2.741 ± 1.62	0.9668 ± 0.090
SR-728	> 50	> 50
SR-687	> 50	> 50

Table.S2. Antiviral activity of the compounds with therapeutic index higher than 100. Vero E6 cell treated with test compounds for two hours was infected with SARS-CoV-2 virus at an MOI of 0.05, then incubated for three days in the presence of compound. Cell viability (protection from virus-induced CPE) was measured with CellTiter-Glo. Cytotoxicity was tested in the same conditions with cell culture media instead of the virus. IC₅₀ and CC₅₀ were calculated with the 4-parameter Logistic model (XLFit fit model 205) and the standard errors (S.E.) were shown.

Figure.S1

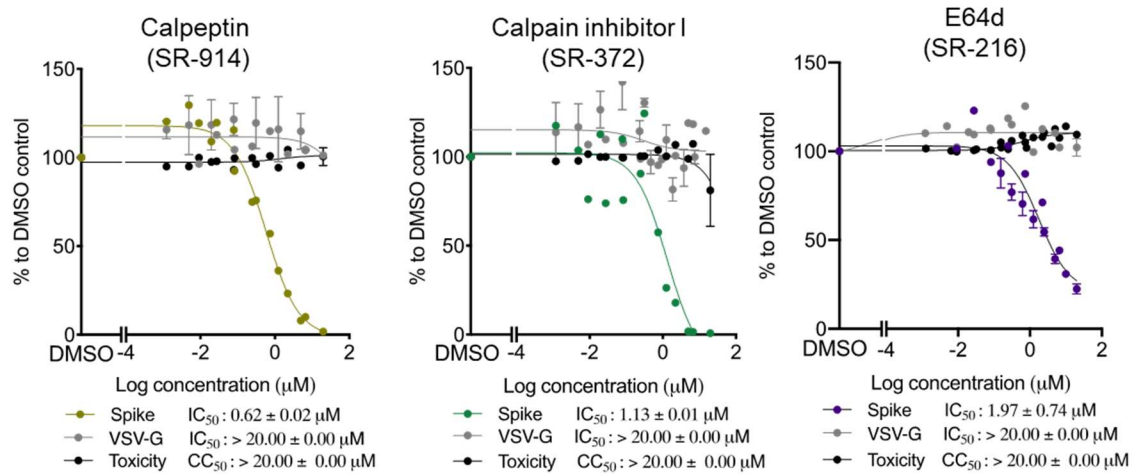


Figure.S1. Activity of SR-914, SR-372 and E64d in Ver0 CCL81 infected with SARS2-S. Cells were incubated with different concentrations of drugs, then infected with SARS2-S or VSV-G. Luciferase was measured 48 hours later, using Bright-Glo. Toxicity was measured, using CellTiter-Glo. E64d was used as control. Shown is the mean \pm SEM of n=2 to 5 independent experiments

Figure.S2

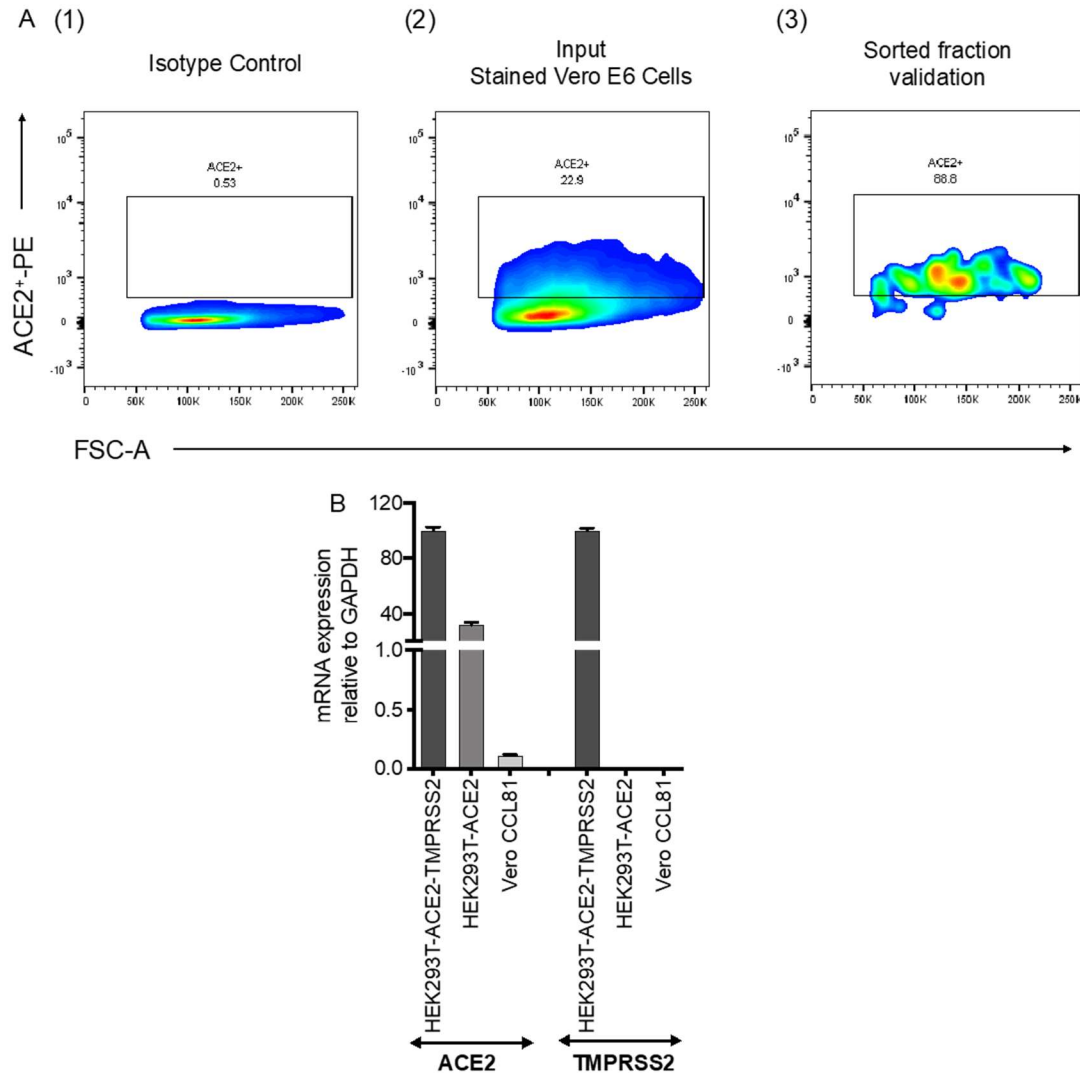


Figure.S2. ACE2 and TMPRSS2 expression in different cell lines. A. Vero E6 cells were stained with Goat anti-Human Phycoerythrin-conjugated ACE-2 Polyclonal Antibody (R&D Systems, Catalog # FAB933P) for 30 min at 4 °C in dark. Cells were then washed with HBSS and suspended in Pre-Sort buffer (BD Biosciences, Cat#56350). ACE2⁺ cells were gated on the basis of Goat IgG Isotype Control (R&D Systems, Catalog # IC108P) (1), and sorted on FACSARIA III. Approximately 23% of the cell population were determined as ACE-positive (2). The cell fraction sorted by the gating was further validated for purity before expansion (3). **B.** Total RNA was extracted, and first-strand cDNA was quantified by qPCR using primers directed to ACE2 or TMPRSS2. Results were normalized as copies of viral mRNA per copy of GAPDH mRNA. The arbitrary value of 100 was assigned to the amount of viral mRNA generated in HEK293T-ACE2-TMPRSS2 cells. Shown is the mean \pm SEM of 2 independent experiments.

Figure.S3

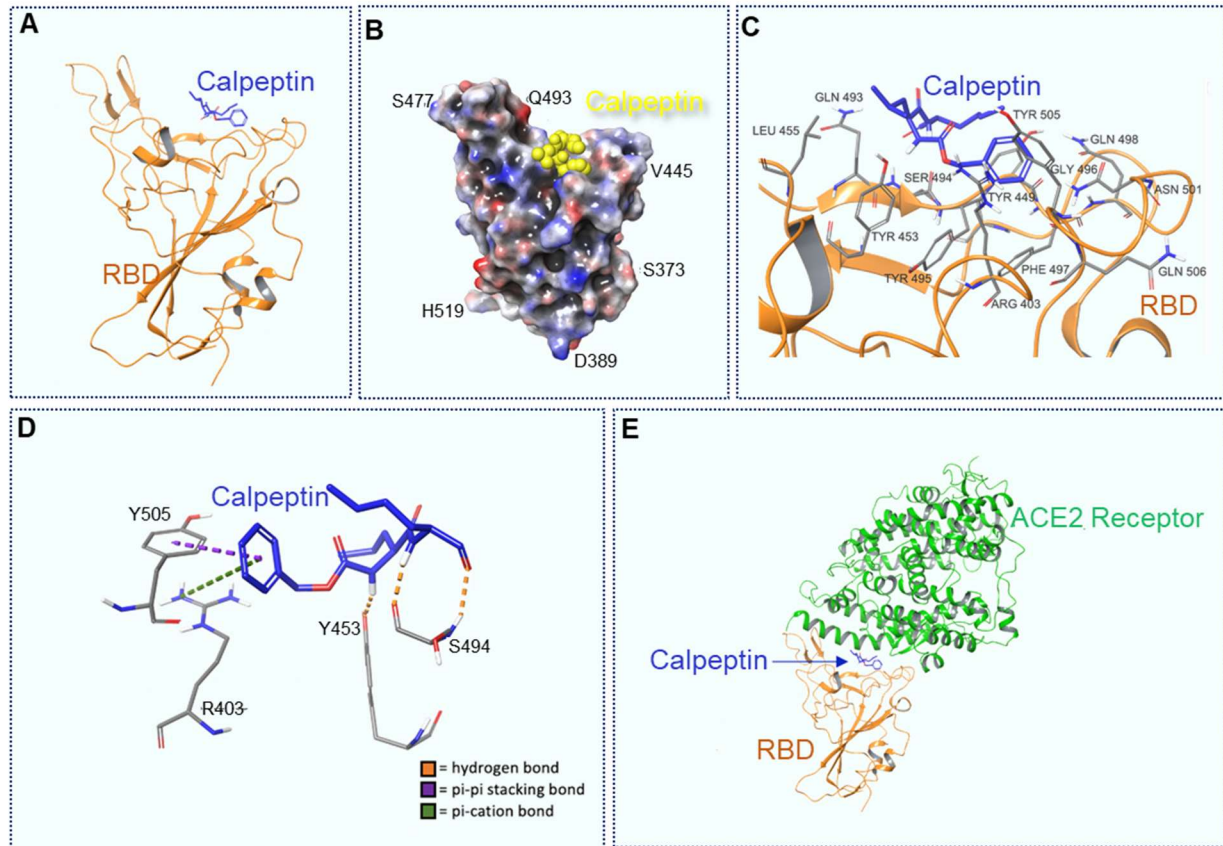


Figure.S3. Docking of Calpeptin to the wild type RBD, using a modified PDB 6M0J structure. A. Calpeptin docked to the RBD. B. 3D view of Calpeptin docked to RBD. Molecular surface colored according to residue electrostatic potential. Calpeptin shown in yellow. C. Calpeptin's interactions with critical residues within the RBD. D. Types of interaction between Calpeptin and RBD. Hydrogen bonds are shown in orange, pi-pi stacking bonds are shown in purple and pi-cation bonds are shown in green. E. Calpeptin docked within the RBD-ACE2 connective interface.

Figure. S4

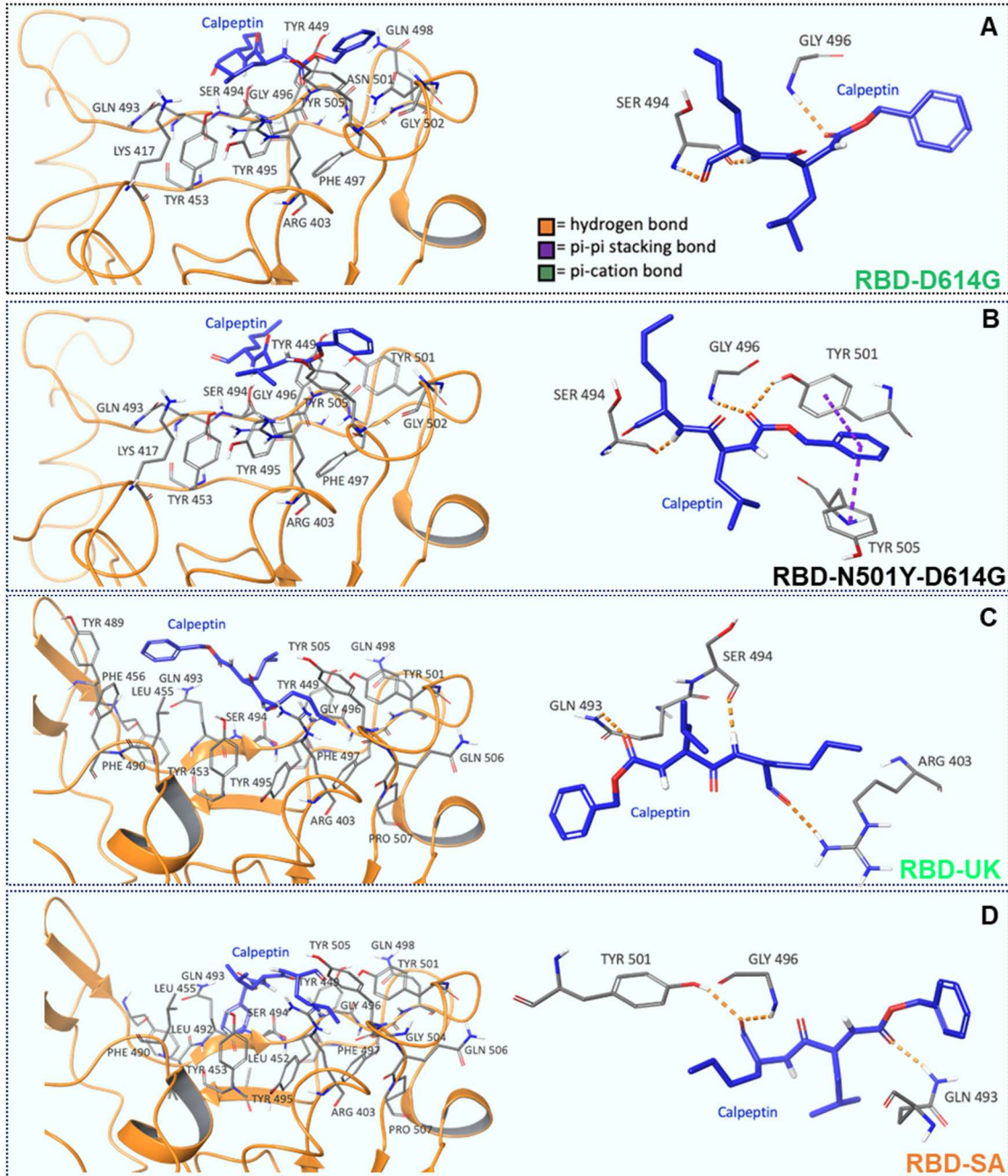
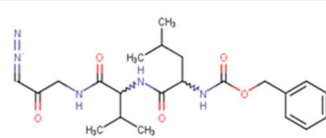


Figure.S4. Docking of Calpeptin to the mutants RBD, using a modified PDB 6M0J and 7KDK structures. Calpeptin docked to the D614G, N501Y-D614G, UK and SA variants of SARS-CoV-2 RBD. Residues and types of interactions are shown.

Figure. S5

A

Compound	Z LVG CHN2, an inactive analog of Calpeptin
Structure	
SARS-2 entry	$> 19.80 \times 10^{-6}$
VSV-G	$> 19.80 \times 10^{-6}$
Toxicity	$> 19.80 \times 10^{-6}$
Glidescore (kCal/mol)	-3.46 vs -4.38 for Calpeptin

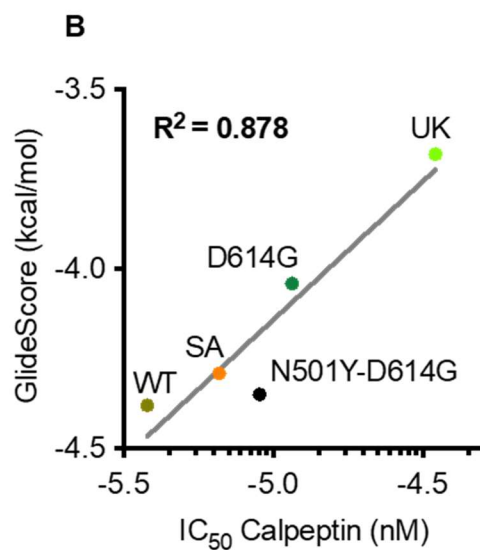


Figure.S5. Docking of Calpeptin to RBDs. A. An inactive analog of Calpeptin binds poorly to wild type RBD. Z LVG CHN2 was tested in SARS-2 entry assay in HTS. Activity and toxicity were measured. Shown is the mean \pm SEM of $n=3$ independent experiments. B. Correlation plot between Glidescore and IC₅₀ of Calpeptin against the different mutants of RBD.